

The temperature dependence of the band gap shrinkage due to the electron–phonon interaction in $\text{Al}_x\text{Ga}_{1-x}\text{As}$

This article has been downloaded from IOPscience. Please scroll down to see the full text article.

2006 J. Phys.: Condens. Matter 18 1687

(<http://iopscience.iop.org/0953-8984/18/5/021>)

View [the table of contents for this issue](#), or go to the [journal homepage](#) for more

Download details:

IP Address: 129.252.86.83

The article was downloaded on 28/05/2010 at 08:54

Please note that [terms and conditions apply](#).

The temperature dependence of the band gap shrinkage due to the electron–phonon interaction in $\text{Al}_x\text{Ga}_{1-x}\text{As}$

Niladri Sarkar and Subhasis Ghosh

School of Physical Sciences, Jawaharlal Nehru University, New Delhi 110067, India

Received 19 October 2005

Published 18 January 2006

Online at stacks.iop.org/JPhysCM/18/1687

Abstract

The photoluminescence spectrum of band edge transitions in $\text{Al}_x\text{Ga}_{1-x}\text{As}$ is studied as a function of temperature and electron concentration. The parameters that describe the temperature dependence redshift of the band edge transition energy are evaluated using different models. We find that a semi-empirical relation based on a phonon dispersion related spectral function leads to an excellent fit to the experimental data.

$\text{Al}_x\text{Ga}_{1-x}\text{As}$ is one of the most important alloy semiconductors [1]. This III–V ternary alloy semiconductor has attracted extensive attention because of its applications in different kinds of heterojunction structures which are used in microelectronic and optoelectronic devices. It has become an important component in high speed electronic devices, such as modulation doped field effect transistors (MODFET) and optoelectronic devices (modulators, detectors and lasers). Because of its excellent lattice match to GaAs substrates, it has also been used as an integral component of various low dimensional heterostructures [2]. Although the growth and characterization of $\text{Al}_x\text{Ga}_{1-x}\text{As}$ and device fabrication based on $\text{Al}_x\text{Ga}_{1-x}\text{As}$ have matured over the last two decades, several fundamental issues such as temperature and doping induced band gap shrinkage (BGS) are still controversial. In addition to fundamental interest, these issues are extremely important for the development and modelling of $\text{Al}_x\text{Ga}_{1-x}\text{As}$ based devices. The temperature induced BGS is observed in experiments via a monotonic redshift of band-to-band (BB) and/or excitonic transitions that are observed in the bulk as well as in low dimensional heterostructures. The temperature dependent band gap $E_g(T)$ varies from relatively weak in the low temperature region to relatively strong in the higher temperature region. There is considerable controversy regarding the temperature induced BGS in $\text{Al}_x\text{Ga}_{1-x}\text{As}$. Most of the previous studies [3–5] on $\text{Al}_x\text{Ga}_{1-x}\text{As}$ have used empirical relations [6, 7], neglecting the role of phonon dispersion [8], to fit the experimental data. There is a large variation of the values of different BGS parameters evaluated using these empirical relations; for example, the most fundamental parameter α , which is $-dE_g(T)/dT$ at the high

temperature limit, varies from 0.6 to 1.4 meV K⁻¹ [3]. Pässler [8, 9] has shown the inadequacy of these empirical relations for temperature induced BGS in different semiconductors.

In this paper, we present the temperature dependence of the BGS in n-type Al_xGa_{1-x}As epitaxial layers. In particular, the role of electron concentration in the different parameters responsible for the BGS has been studied. The results are compared with different empirical and semi-empirical models for the BGS. We have used n-type Al_xGa_{1-x}As epilayers which are grown by metal–organic chemical vapour epitaxy (MOCVD) on semi-insulating or n-type GaAs substrates. Se is chosen as the dopant for its high solubility, low compensation yielding the highest doping level and minimum DX centre related problems [10]. The active Al_xGa_{1-x}As layers are separated from the GaAs substrate by an undoped spacer layer to avoid any two-dimensional (2D) effects. The AlAs mole fraction x of our samples is 0.22. The thicknesses of all the Al_{0.22}Ga_{0.78}As layers were about 2–4 μm. The electron concentrations, ranging from 3×10^{16} to 3×10^{18} cm⁻³, were determined by Hall measurements. The photoluminescence (PL) spectra were collected in the wavelength region of 630–800 nm. The samples were kept in a closed cycle He refrigerator and were excited with the 488 nm laser line of an Ar ion laser. The PL signal was collected into a monochromator and detected with a Si detector.

Figure 1 shows the evolution of room temperature and low temperature PL spectra of n-type Al_{0.22}Ga_{0.78}As as a function of the electron concentration. The sample with the lowest electron concentration of 3.5×10^{16} cm⁻³ was sample 1A; the dominant peak at 1.842 eV is due to a bound exciton (BE) and the broad peak at 1.822 eV is due to free-to-bound (FB) and donor–acceptor (DAP) related transitions. A high energy shoulder at 1.847 eV is due to either band-to-band (BB) or free exciton (FE) cases. As the electron concentration is slightly increased to 4.5×10^{16} cm⁻³ in sample 1B, very similar PL spectra are observed in the case of sample 1B, but as the electron concentration increases to 1.3×10^{17} cm⁻³, for sample 1C a BB peak appears in lieu of BE and FE peaks due to the quenching of free excitons and the screening of impurity potential. As the electron concentration is slightly increased to 3.1×10^{17} cm⁻³, very similar PL spectra are observed in the case of sample 1D. Now, as the electron concentration is further increased to 8.3×10^{17} cm⁻³ in sample 1E, an extra high energy peak at 1.858 eV in addition to the BB, FB and DAP peaks is observed. Again, as the electron concentration is further increased to 9.6×10^{17} cm⁻³ slightly in sample 1F, PL spectra similar to those of 1E are observed. But when the electron concentration is further increased to 2.8×10^{18} cm⁻³ in sample 1G, the high energy peak at 1.858 eV disappears. The energetic positions and saturation behaviour have revealed the identification of these peaks [11]. Hence, the transitions due to FE, BE, FB and DAP are observed in samples with low electron concentration. As the electron concentration is increased by an order of magnitude, FE and BE peaks are replaced with BB transition ones, but FB and DAP peaks are observed for all samples. Typical BB transitions are observed in room temperature PL spectra (figure 1), which are characterized by a Maxwell–Boltzmann lineshape [12] on the high energy side and a relatively sharp cut-off on the low energy side caused by an $(E_g - E)^{1/2}$ dependence. It is clear that BB peaks shift towards lower energy as the electron concentration increases. The redshift of the BB peak is also observed at low temperature. This redshift is due to heavy doping induced band gap narrowing caused by correlation and exchange interaction among carriers [11, 13]. The extra high energy peak at 1.858 eV has not been observed in previous PL studies on Al_xGa_{1-x}As [11]. The variation of the band gap in Al_xGa_{1-x}As due to alloy fluctuation determined by scanning the sample with the BE peak energy has been found to be small (~ 0.7 meV cm⁻¹) across the sample and this fluctuation corresponds to a variation of x of less than 0.001 cm⁻¹ and rules out the possibility of an energetic shift of BB or excitonic transition towards higher energy due to band gap variations. The energetic position of this new peak is almost 20 meV above the band gap. We have found that the position of the Fermi level in samples with electron concentrations of

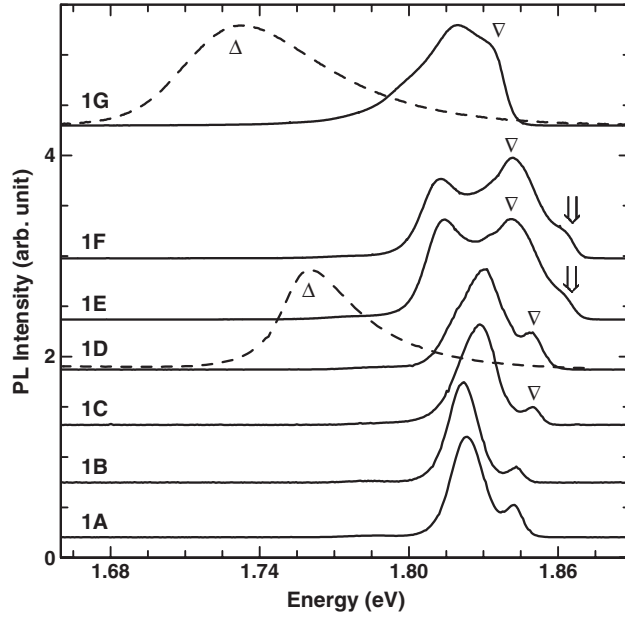


Figure 1. Evolution of PL spectra of $\text{Al}_{0.22}\text{Ga}_{0.78}\text{As}$ as a function of electron concentration. Solid lines (for samples 1A, 1B, 1C, 1D, 1E, 1F, 1G) represent PL spectra at $T = 1.8$ K and dashed lines (for samples 1D and 1G) represent PL spectra at $T = 300$ K. The peaks at 1.842 eV and 1.822 eV for samples 1A and 1B are due to BE and DAP, respectively. The peaks at around 1.83 eV for samples 1C and 1D are due to DAP and FB and cannot be resolved for these samples. The peaks at 1.813 eV for samples 1E and 1F are due to DAP and FB and cannot be resolved for these samples. The peak at 1.82 eV for sample 1G is due to FB and DAP and can be observed as a weak shoulder. Triangles and inverted triangles indicate the spectral positions of band-to-band transitions at $T = 300$ K and 1.8 K, respectively. Inverted arrows (\Downarrow) indicate the spectral position of the FES feature in the PL spectra. The electron concentrations in samples 1A, 1B, 1C, 1D, 1E, 1F and 1G are $3.5 \times 10^{16} \text{ cm}^{-3}$, $4.5 \times 10^{16} \text{ cm}^{-3}$, $1.3 \times 10^{17} \text{ cm}^{-3}$, $3.1 \times 10^{17} \text{ cm}^{-3}$, $8.3 \times 10^{17} \text{ cm}^{-3}$, $9.6 \times 10^{17} \text{ cm}^{-3}$ and $2.8 \times 10^{18} \text{ cm}^{-3}$, respectively.

8.3×10^{17} – $9.6 \times 10^{17} \text{ cm}^{-3}$ is around 20 meV above the minimum of the conduction band at low temperature (< 10 K). The high energy peak is completely quenched for sample (1G) with $2.8 \times 10^{18} \text{ cm}^{-3}$ electron concentration, but BB, FB and DAP peaks are present, as shown in figure 1. We have shown [13] that this high energy peak is due to a Fermi edge singularity (FES), which arises due to multiple scattering of electrons near the Fermi edge caused by the photogenerated holes localized by alloy fluctuation and perhaps also by charged dopants in $\text{Al}_x\text{Ga}_{1-x}\text{As}$.

Hence, by varying the background electron concentration, it is possible to study the temperature dependence of BB or excitonic transitions separately. The temperature dependence of the PL spectra of two n-type $\text{Al}_{0.22}\text{Ga}_{0.78}\text{As}$ samples (1D and 1G) with different electron concentrations is shown in figure 2, which shows a maximum redshift of about 92 meV as temperature increases from 10 to 300 K. An appropriate fitting function is required to obtain material specific parameters from the experimentally measured $E_g(T)$. First-principles theoretical calculation of the temperature dependent band structure is an extremely complicated problem and the Car–Parrinello approach [14], which is the best one could do now, does not provide parameters which can be compared with experimental results, so different empirical and semi-empirical relations are used to explain the experimental data. There are two sets of

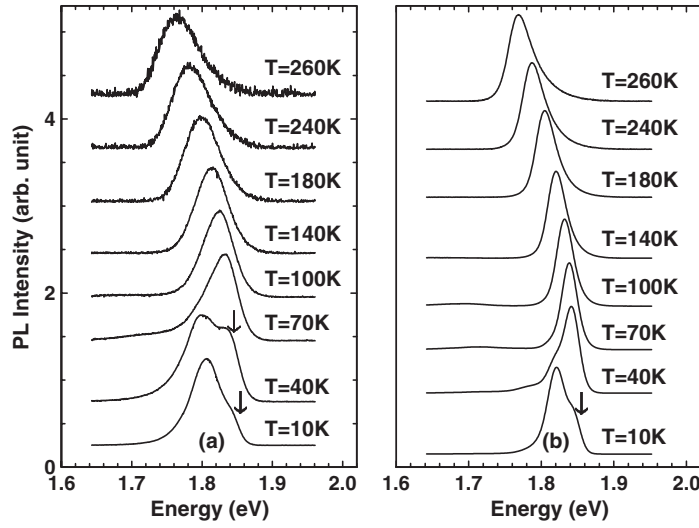


Figure 2. PL spectra of the band edge transition at different temperatures from 10 to 300 K in $\text{Al}_{0.22}\text{Ga}_{0.78}\text{As}$ with electron concentrations of (a) $2.8 \times 10^{18} \text{ cm}^{-3}$ and (b) $3.1 \times 10^{17} \text{ cm}^{-3}$. The inverted arrows (\downarrow) point to the peak of the BB transition at low temperature.

fitting function for $E_g(T)$ in the literature: (i) empirical relations proposed by Varshni [6] and Viña *et al* [7] and (ii) semi-empirical relations based on the electron–phonon spectral function $f(\epsilon)$ and the phonon occupation number $n(T)$; ϵ is the phonon energy.

The most frequently used empirical relation for numerical fittings of $E_g(T)$ was first suggested by Varshni [6] and is given by

$$E_g(T) = E_g(0) - \frac{\alpha T^2}{\beta + T} \quad (1)$$

where $E_g(0)$ is the band gap at 0 K, α is the $T \rightarrow \infty$ limiting value of the BGS coefficient $dE_g(T)/dT$ and β is a material specific parameter. This model represents a combination of a linear high temperature dependence with a quadratic low temperature asymptote for $E_g(T)$. There have been several problems with this relation, for example (i) this relation gives negative values of α and β in the case of wide band gap semiconductors [6, 15], (ii) β is a physically undefinable parameter believed to be related to the Debye temperature Θ_D of the semiconductor, but this connection has been doubted in several cases [9] and it has been shown that this relation cannot describe the experimental data for $E_g(T)$ even for GaAs [16]. Figures 3(a) and 4(a) show the comparison of the experimental $E_g(T)$ with Varshni's relation [6]. We have obtained the values of α in the range of 0.57–0.62 meV K⁻¹ and β in the range of 300 to 315 K. It is clear that though the fitting is good in the low temperature region (<40 K), it is not so good in the intermediate (~ 100 K) and high temperature regions (>200 K).

Viña *et al* [7] first emphasized that the total BGS $\Delta E_g(T) = E_g(0) - E_g(T)$ is proportional to the average phonon occupation number $\bar{n}(T) = [\exp(\frac{\epsilon}{k_B T}) - 1]^{-1}$ and proposed an empirical relation which can be expressed as

$$E_g(T) = E_g(0) - \frac{\alpha_B \Theta_B}{\exp(\frac{\Theta_B}{T}) - 1} \quad (2)$$

where $\alpha_B = \frac{2a_B}{\Theta_B}$, a_B represents the strength of the electron–phonon interaction, $\Theta_B = \frac{\hbar\omega_{\text{eff}}}{k_B}$

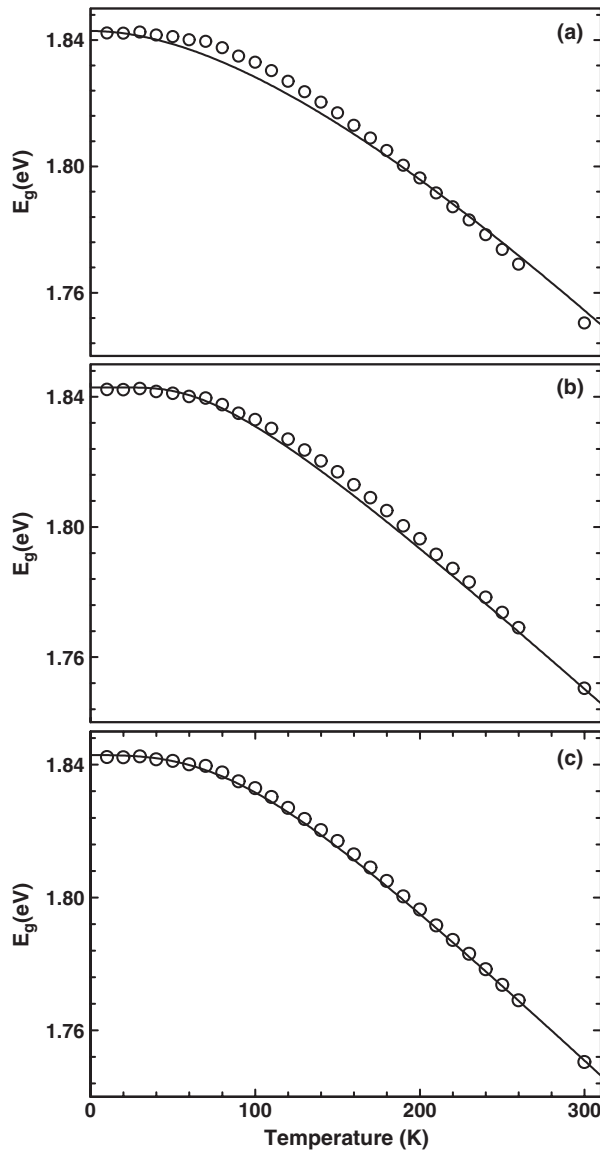


Figure 3. Temperature dependence of the peak position due to the BB transition in $\text{Al}_{0.22}\text{Ga}_{0.78}\text{As}$ with electron concentration $3.1 \times 10^{17} \text{ cm}^{-3}$. Solid lines are fits to the experimental data with (a) equation (1), (b) equation (2) and (c) equation (4).

represents some effective phonon temperature and ω_{eff} is the effective phonon frequency. Although this phenomenological model gave reasonable fittings of $E_g(T)$ in different semiconductors, there are also several problems with this relation, for example, (i) at low temperature, this model shows a plateau behaviour of $E_g(T)$, which is not observed experimentally, (ii) at higher temperature (≥ 50 K), this model predicts $\Delta E_g(T) \propto \exp(-\Theta_B/T)$, but in most cases $\Delta E_g(T) \propto T^2$ is observed experimentally, (iii) it has been shown that this relation cannot describe the experimental data for $E_g(T)$ even for GaAs [16]. Figures 3 (b) and 4(b) show the comparison of experimental $E_g(T)$ with Viña's relation. We have obtained the values of Θ_B in the range of 220 K to 245 K and α_B in the range of 0.42–0.46 meV K⁻¹. This gives much better fitting than Varshni's relation in the high temperature region.

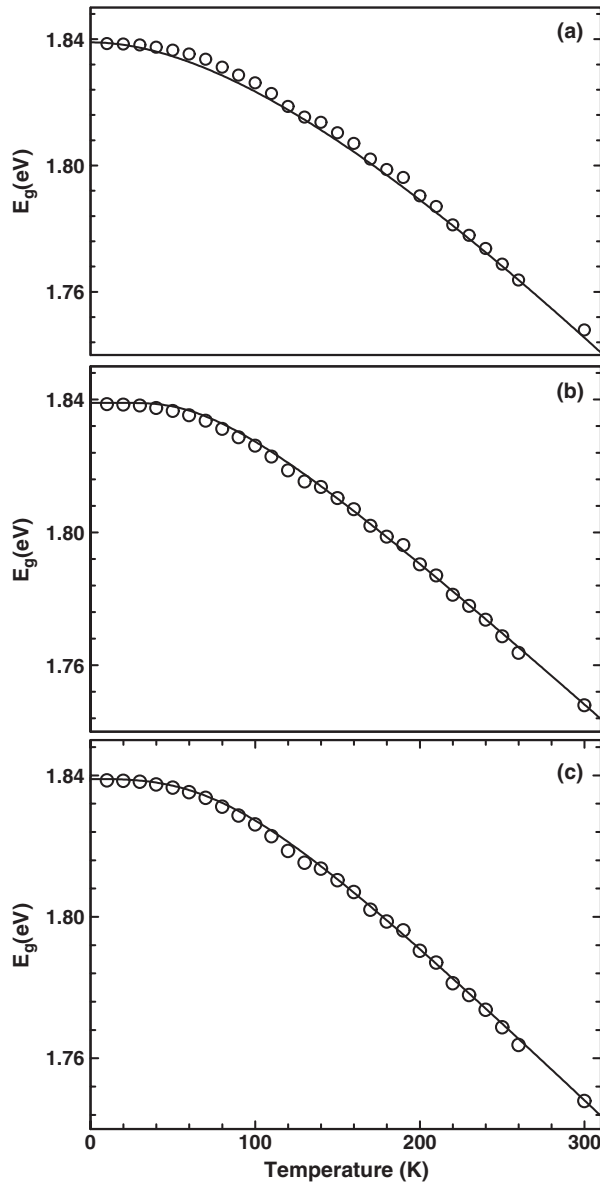


Figure 4. Temperature dependence of the peak position due to the BB transition in $\text{Al}_{0.22}\text{Ga}_{0.78}\text{As}$ with the electron concentration $2.8 \times 10^{18} \text{ cm}^{-3}$. Solid lines are fits to the experimental data with (a) equation (1), (b) equation (2) and (c) equation (4).

As mentioned earlier, it can be shown that the contribution of individual phonon modes to the temperature induced BGS is related to the average phonon occupation number $\bar{n}(T)$ and the electron–phonon spectral function $f(\epsilon)$. Essentially, $E_g(T)$ can be analytically derived from the expression

$$E_g(T) = E_g(0) - \int d\epsilon f(\epsilon) \bar{n}(\epsilon, T). \quad (3)$$

The electron–phonon spectral function $f(\epsilon)$ is not known *a priori* and is extremely complicated to calculate from first principles. The other option is to use a different approximate function for $f(\epsilon)$ to derive the temperature dependence of the BGS. It has been emphasized conclusively [8, 9] that the indispensable prerequisite for estimation of different parameters

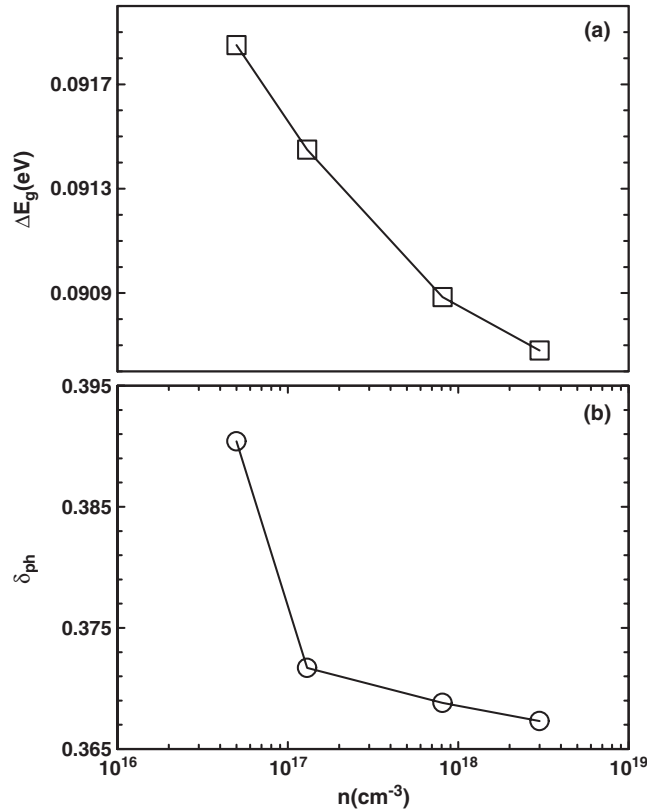


Figure 5. Variation of (a) the total redshift due to the BGS, $\Delta E_g = E_g(10 \text{ K}) - E_g(300 \text{ K})$, and (b) the phonon dispersion coefficient δ_{ph} with the electron concentration n in $\text{Al}_{0.22}\text{Ga}_{0.78}\text{As}$ samples. Solid lines are guides for the eyes.

obtained from the experimentally measured $E_g(T)$ is the application of an analytical model that accounts for the phonon energy dispersion. The BGS results from the superposition of contributions made by phonons with substantially different energies, beginning from the zero-energy limit for acoustic phonons up to the cut-off energy for the optical phonons. The basic features of the phonon dispersion δ_{ph} and the relative weights of their contributions to $E_g(T)$ may vary significantly from one material to another. The curvature of the nonlinear part of $E_g(T)$ is closely related to the actual position of the centre of gravity, $\bar{\epsilon}$ ($\epsilon = \hbar\omega$), and the effective width $\Delta\epsilon$ of the relevant spectrum of phonon modes that make a substantial contribution to $E_g(T)$, and this has been quantified by the phonon dispersion coefficient δ_{ph} ($=\frac{\Delta\epsilon}{\bar{\epsilon}}$). It has been shown [15, 17] that the above two empirical models (equations (1) and (2)) represent the limiting regimes of extremely large $\delta_{\text{ph}} \approx 1$ in the case of Varshni's relation or extremely small $\delta_{\text{ph}} \approx 0$ in the case of Viña's relation. Both these models contradict physical reality for most semiconductors, whose phonon dispersion coefficients vary between 0.3 and 0.6 [15, 17]. Several analytical models have been presented using different forms of the spectral function $f(\epsilon)$. Pässler [8] has proposed the most successful model, which has a power-law-type spectral function, $f(\epsilon) = \nu \frac{\alpha_p}{k_B} \left(\frac{\epsilon}{\epsilon_0}\right)^\nu$, and the cut-off energy ϵ_0 , which is given by $\epsilon_0 = \frac{\nu+1}{\nu} k_B \Theta_p$. Here, ν represents an empirical exponent whose magnitude can be estimated by fitting the experimental data $E_g(T)$. Inserting the spectral function $f(\epsilon)$ and

cut-off energy ϵ_0 into the general equation for the BGS (equation (3)), Pässler [8] obtained an analytical expression for $E_g(T)$, given by

$$E_g(T) = E_g(0) - \frac{\alpha_p \Theta_p}{2} \left[\sqrt[p]{1 + \left(\frac{2T}{\Theta_p}\right)^p} - 1 \right] \quad (4)$$

where $p = \nu + 1$ and α_p is the $T \rightarrow \infty$ limit of the slope $dE_g(T)/dT$, Θ_p is comparable with the average phonon temperature [8], $\Theta_p \approx \bar{\epsilon}/k_B$ and the exponent p is related to the material specific phonon dispersion coefficient δ_{ph} , by the relation $\delta_{ph} \approx 1/\sqrt{p^2 - 1}$. Depending on the value of δ_{ph} , there are regimes of large and small dispersion which are approximately represented within this model by exponents $p < 2$ and $p \geq 3.3$ respectively. Figures 3(c) and 4(c) show the comparison of experimental $E_g(T)$ with equation (4). We obtain an excellent fit to the experimental data. The value of α_p obtained here is in the range of 0.40–0.45 meV K⁻¹ and the value of Θ_p in the range of 210–230 K. The value of the exponent p which is related to the material specific degree of phonon dispersion is obtained between 2.75 to 2.90 for different Al_{0.22}Ga_{0.78}As samples. If we look very closely at the fitting obtained from Viña's (equation (2)) and Pässler's relation (equation (4)), we find that Pässler's relation gives a much better fitting to all the experimental data points.

We have also calculated the total redshift $\Delta E_g = E_g(10 \text{ K}) - E_g(300 \text{ K})$ for all the Al_{0.22}Ga_{0.78}As samples. Figure 5 shows the total redshift ΔE_g and the phonon dispersion δ_{ph} decrease with increase of the electron concentration in Al_{0.22}Ga_{0.78}As. This can be explained in terms of the screening of the relevant electron–phonon interaction with higher electron concentration in the heavily doped samples. It can be noted by comparing figures 3 and 4 that the fitting with Viña's relation [7] is substantially improved as the electron concentration is increased by an order of magnitude. This can again be explained as due to the quenching of the electron–phonon interaction by the higher background electron concentration.

In conclusion, we have measured the temperature induced BGS in Al_{0.22}Ga_{0.78}As using PL spectroscopy. The importance of electron–phonon interaction for the BGS has been established. It has been found that a phonon dispersion based semi-empirical relation is required to explain the experimental data. Screening of the electron–phonon interaction is responsible for the decrease of the temperature induced BGS in samples with higher electron concentration.

References

- [1] Adachi S 1993 *Properties of Aluminium Gallium Arsenide* (London: Institution of Electrical Engineers)
- [2] Weisbuch C and Vinter B 1991 *Quantum Semiconductor Structures* (Boston: Academic)
- [3] Logothetidis S, Cardona M and Garriga M 1991 *Phys. Rev. B* **43** 11950
- [4] Allali M E *et al* 1993 *Phys. Rev. B* **48** 4398
- [5] Newmann H *et al* 1992 *Phys. Status Solidi b* **171** K79
- [6] Varshni Y P 1967 *Physica* **34** 149
- [7] Viña L, Logothetidis S and Cardona M 1984 *Phys. Rev. B* **30** 1979
- [8] Pässler R 1999 *Phys. Status Solidi b* **216** 975
- [9] Pässler R 2002 *Phys. Rev. B* **66** 085201
- [10] Gibart P and Bismajji P 1990 *Physics of DX Centers in GaAs Alloys* ed J C Bourgoin (Vaduz: Trans Tech)
- [11] Pavesi L and Guzzi M 1980 *J. Appl. Phys.* **51** 2634
- [12] Ghosh S 2000 *Phys. Rev. B* **62** 8053
- [13] Sarkar N and Ghosh S 2005 *Phys. Rev. B* **71** 233204
- [14] Car R and Parrinello M 1985 *Phys. Rev. Lett.* **55** 2471
- [15] Pässler R 2000 *J. Appl. Phys.* **88** 2570
- [16] Grilli E, Guzzi M, Zamboni R and Pavesi L 1992 *Phys. Rev. B* **45** 1638
- [17] Pässler R 2001 *J. Appl. Phys.* **89** 6235